

# CRARP 25-02 OBSERVATIONAL STUDY OF A DIURNAL MESOSCALE CONVECTIVE COMPLEX

David Novak<sup>1</sup> and Edward Shimon  
National Weather Service Forecasting Office  
Duluth, Minnesota

## 1. Introduction

The Mesoscale Convective Complex (MCC) has been described by Maddox (1980), Bosart and Sanders (1981), and Maddox (1983) as a unique class of intense convection organized on the meso-alpha scale, which occurs primarily in the central United States during the convective season. Fritsch et al. (1981) and Wetzel (1983) showed that MCCs produce locally intense rainfall, large hail, and damaging winds, requiring coincident operational warnings of both severe weather and flash flooding.

In contrast to most convection MCCs are distinctly nocturnal (Maddox 1983). Augustine and Caracena (1994) as well as McAnelly and Cotton (1986) have shown that MCCs commence from afternoon thunderstorms in the western Great Plains that organize and continue to develop at night into MCCs. Physically, this nocturnal preference has been linked to the Low Level Jet (LLJ) (Maddox 1980; Wetzel 1983; Maddox 1983), which enhances warm air advection and the flux of moist, unstable air into the system. Composites from Maddox (1983) confirm that MCCs reach maximum size around local midnight, corresponding with the strongest LLJ, and weaken during the morning hours when the LLJ typically weakens (Fig. 1).

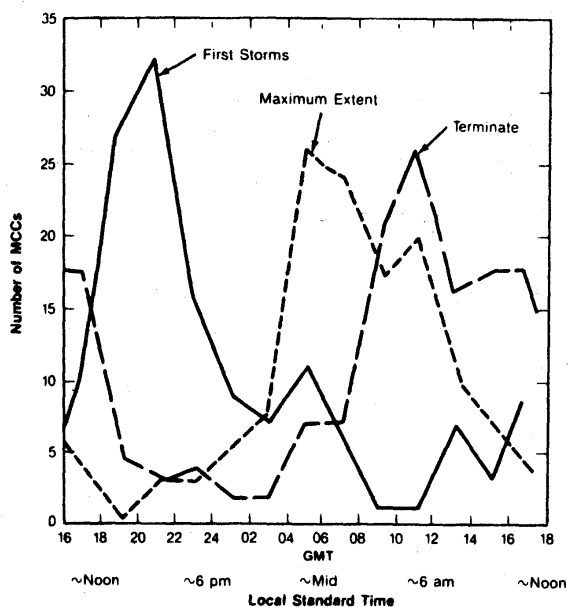


Fig. 1. Composites of MCCs from Maddox (1983) showing the the time of initiation (solid), maturity (short dash), and termination (long dash). (Adopted from Maddox 1983).

In contrast to this widely confirmed characteristic of MCCs, convection on 14 August 2000 organized during the early morning in eastern North Dakota, reached maximum intensity and organization *during the day* across northern Minnesota and northern Wisconsin, and then slowly weakened during the early morning hours of 15 August in central Wisconsin. The timing of this event is completely out of phase with Maddox (1983), and contributed to its unpredicted magnitude and timing (personal communication with the Duluth National Weather Service Forecasting Office (NWSFO)). Examination reveals this system closely conforms to the *frontal* pattern for flash floods described by Maddox et al. (1979). This study examines the mesoscale and synoptic evolution of the 14 August event, contrasting it with the *frontal* pattern presented by Maddox et al. (1979). Special attention will be given to the synoptic and mesoscale environment that promoted regenerative development during the day.

<sup>1</sup> Current affiliation: Department of Earth and Atmospheric Sciences, State University of New York (SUNY) at Albany

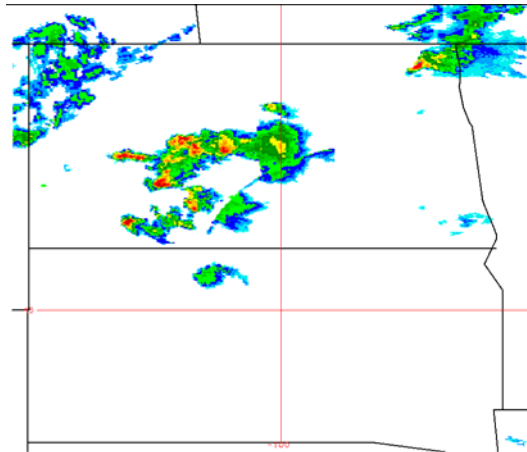
## 2. Data and methodology

Data used for the 14 August 2000 case include manual analyses of surface observations and upper air data obtained from the surface and radiosonde network. Standard National Centers for Environmental Prediction (NCEP) synoptic maps are used to describe the synoptic environment prior, during, and after maximum development. Composite radar data with a 2 km resolution were acquired from the Cooperative Program for Operational Meteorology, Education, and Training (COMET). The 1200 UTC and 1800 UTC 14 August and 0000 UTC 15 August National Centers for Environmental Prediction (NCEP) Eta model analysis fields were used to calculate derived kinematic and dynamic fields with the aid of the General Meteorological Package (GEMPAK). Soundings and cross-section analyses were created by GEMPAK. In an effort to obtain optimal temporal resolution of the lower tropospheric wind evolution, data from the Wood Lake, Minnesota wind profiler from 1200 UTC 14 August until 0600 UTC 15 August was used. Corfidi vectors were calculated manually by the procedure outlined in Corfidi et al. (1996). **Storm Data** (NOAA 2000) was referenced to document severe weather reports.

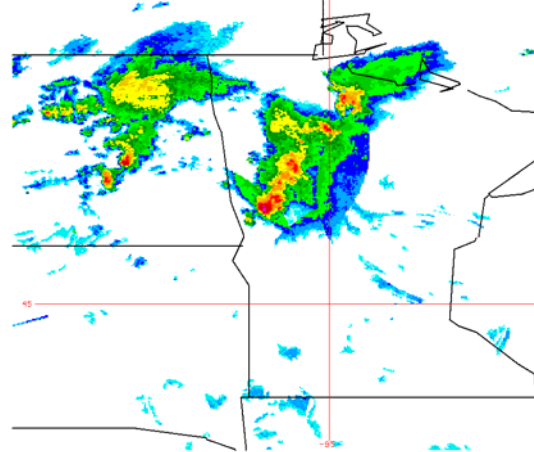
### 2. Case description

#### a. Evolution of the event

Radar imagery from 14 and 15 August 2000 (Fig. 2) show the evolution of the MCC. Between 0000 UTC and 0600 UTC 14 August (times and dates will hereafter be abbreviated as “date/time UTC”) convection initiated in eastern Montana and moved east. By 14/06 the convection organized into a MCS in central North Dakota. The composite radar image at this same time (Fig. 2a) collaborates the position of the MCS. The system continued to organize as it moved across North Dakota, producing large hail from northeast North Dakota into west central Minnesota (**Storm Data** NOAA 2000). Lighter stratiform rain was observed in the extensive cloud shield across northern Minnesota. The 14/12 composite radar image (Fig. 2b) shows two areas of convection – the strongest in west-central Minnesota, and new development further northwest in North Dakota. During the morning hours the convection in Minnesota dissipated – consistent with diurnal expectations; however, convection in North Dakota continued to organize and intensify.



a) 14/0600



b) 14/1200

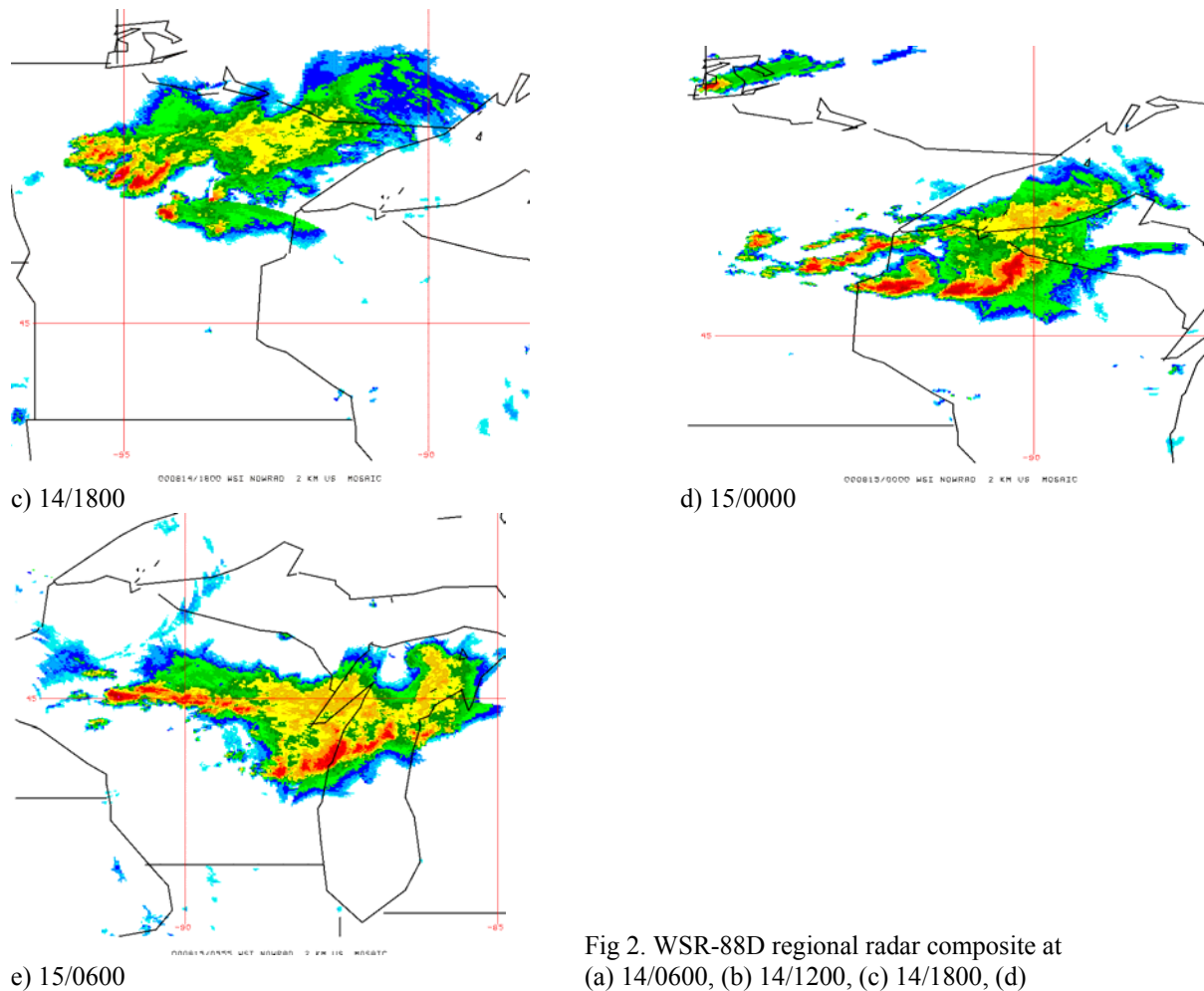


Fig 2. WSR-88D regional radar composite at (a) 14/0600, (b) 14/1200, (c) 14/1800, (d) 15/0000, and (e) 15/0600.

From 14/12 regenerative storm development was noted on the western flank of the convection, with severe cells training over the same areas. The 14/18 radar image (Fig. 2c) shows a series of severe cells on the southwest flank of the system. Subsequent hail accumulation totaled several inches, and flash flooding commenced (Storm Data). Although direct cloud top temperature data were not obtained, a subjective assessment employing the definition set by Maddox (1983) designated the MCS as a MCC at 14/18.

From 14/18 until 15/00 (Fig. 2c and 2d) continued regenerative storm development occurred on the southwest flank of the system. Cass county in Minnesota was under verified severe thunderstorm warnings for over six hours, with associated rainfall reported over 8 cm. In addition to large hail, severe winds toppled trees killing one person in the county around 14/20 (Storm Data).

From 15/00 until 15/06 (Fig. 2e) the MCC continued producing large hail, damaging winds, and flooding rains on the southwest flank of the system as it moved southeast into Wisconsin. The 15/00 radar composite (Fig. 2d) attests to the severity of the convection. A bow echo in north-central Wisconsin exhibiting a rear inflow notch and book-end vortices is evident. Although the system showed regenerative growth (note the new cells in central Minnesota), it was not as prominent as in earlier times. After 15/06 the MCC quickly lost strength as it progressed briskly to the east. A total of 66 warnings were issued by the Duluth WFO.

*b. The synoptic environment*

Analysis of the 14/00 and 14/12 500 hPa geopotential height and vorticity fields (Fig. 3) shows a positively tilted trough in western Canada swinging east into the Canadian Prairie Provinces by 14/12 (Fig. 3 upper left panel). A broad ridge is evident over the central U.S. It should be noted that this trough over ridge pattern has been documented as a classic derecho set-up (the meteorological “ring of fire”). The 15/00 (Fig. 3 upper right panel) and 15/12 (Fig. 3 lower left panel) analyses show the continued eastward progression of the trough on top of the large-scale ridge.

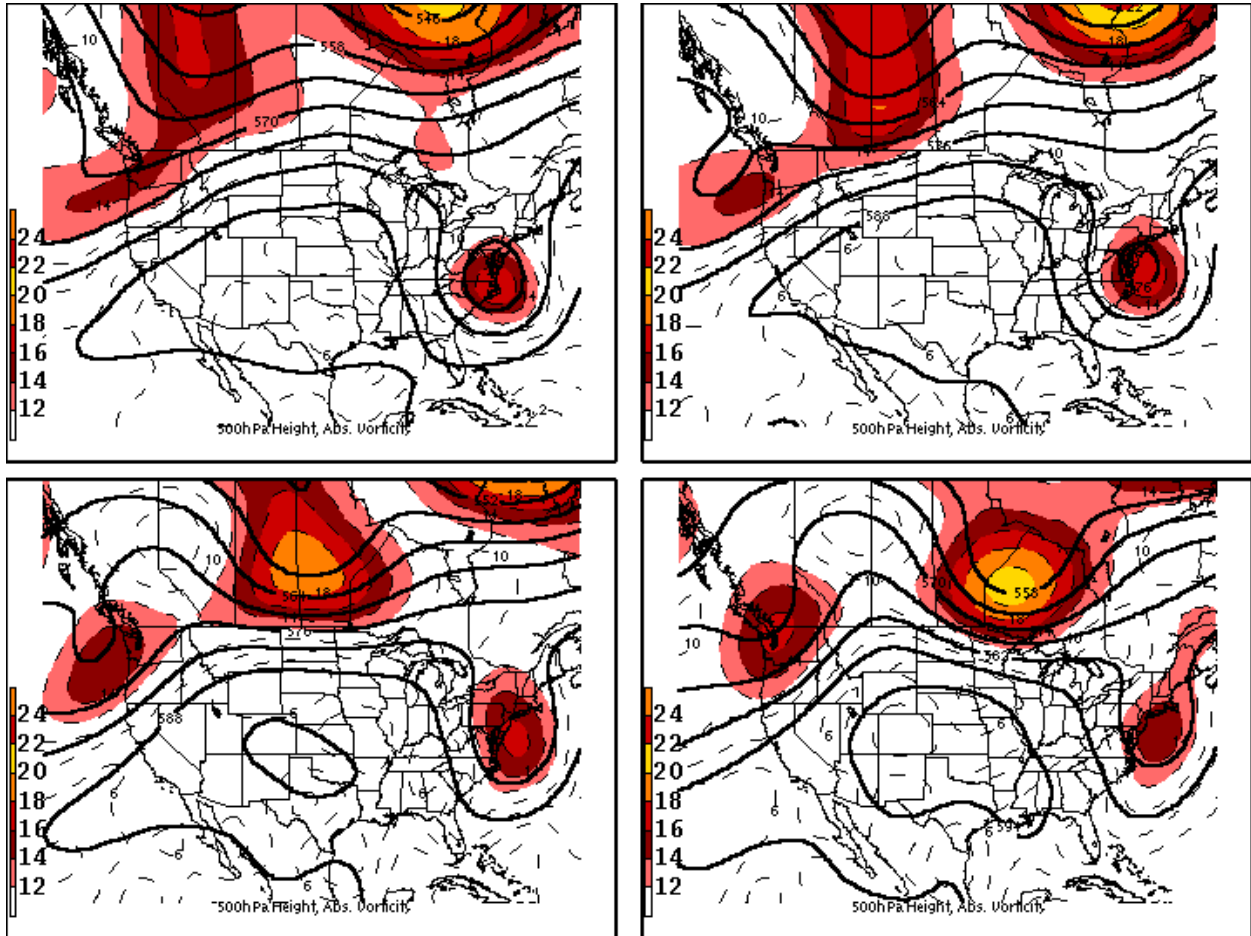


Fig. 3. 500 hPa heights (solid lines) and vorticity (dashed lines, shaded  $>12 \text{ s}^{-1}$ ) at 14/00 (upper left panel), 14/12 (upper right panel), 15/00 (lower left panel), and 15/12 (lower right panel).

The 14/00 (Fig 4 upper left panel) and 14/12 (Fig 4 upper right panel) 850 hPa maps suggest warm air advection into the northern Great Plains which shifts east into eastern North Dakota and Minnesota by 14/12. Note the development of a 25 kt LLJ by 14/12 evident from northern Texas into Minnesota. This LLJ is distinctly apparent from the 14/12 Aberdeen (ABR) sounding (Fig. 5a), which shows 21.5 m/s south winds at 925 hPa. By 15/00 (Fig. 4 lower left panel) the 850 hPa wind maximum has shifted eastward. Note the 25 kt southwesterly flow from eastern Kansas into east central Minnesota. Also evident is the continued warm air advection into Wisconsin. By 15/12 (Fig. 4 lower right panel) cold advection is dominating Minnesota and Wisconsin, with no evidence of a LLJ into the lower Great Lakes.

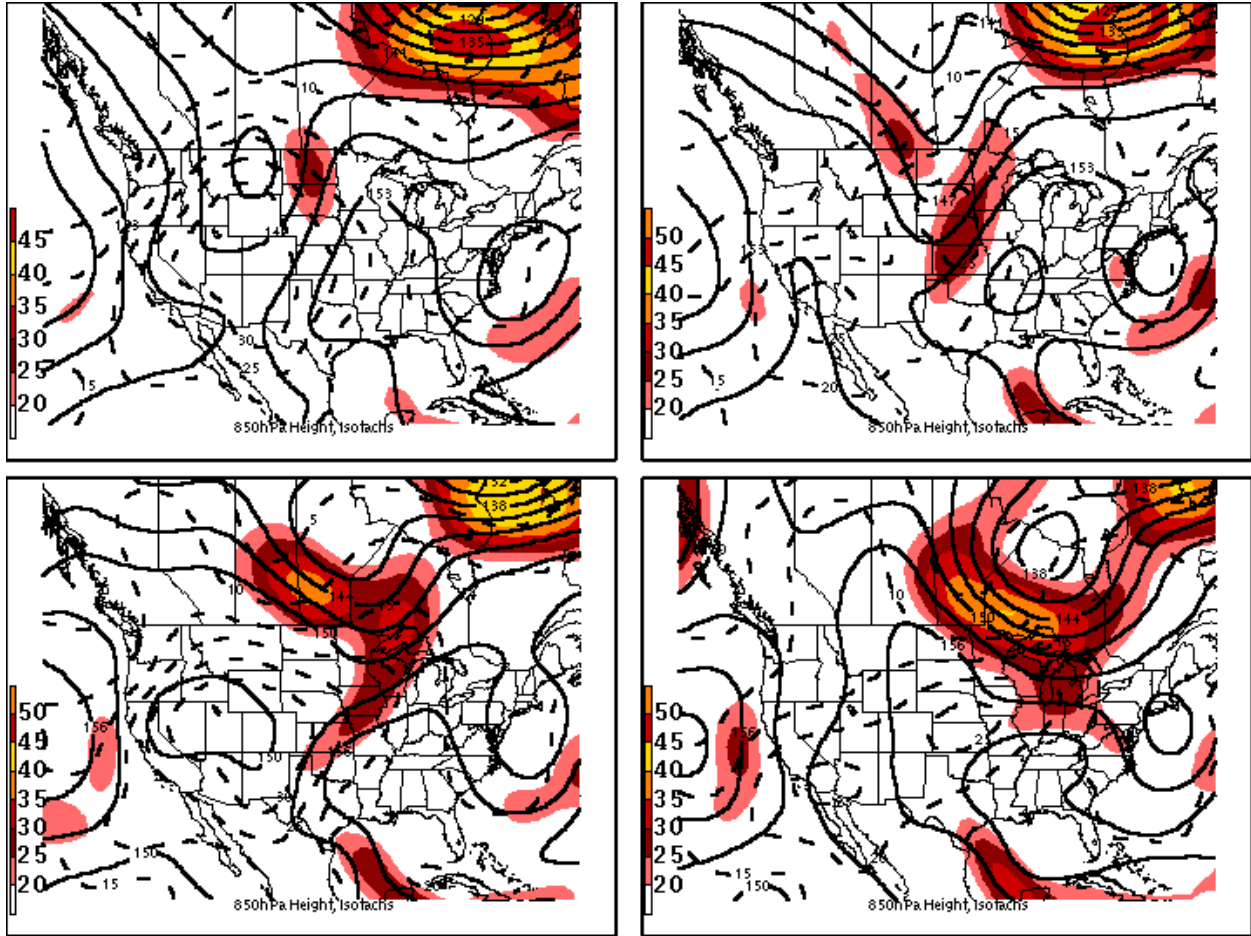
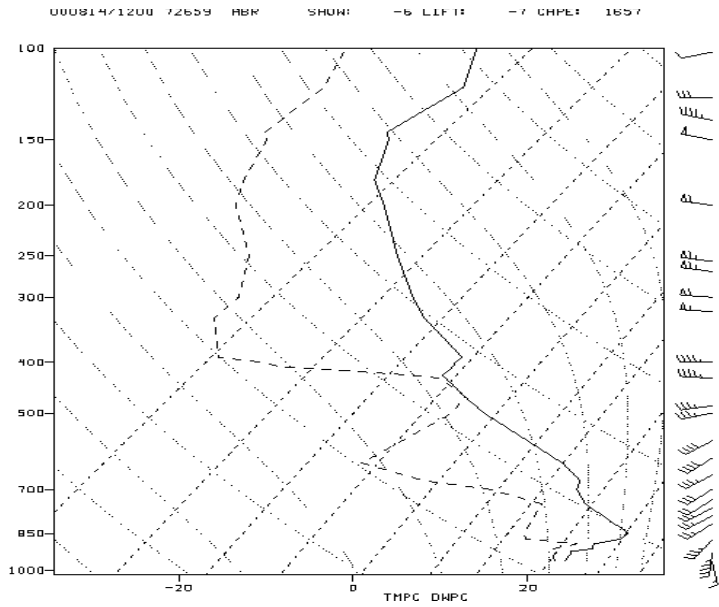
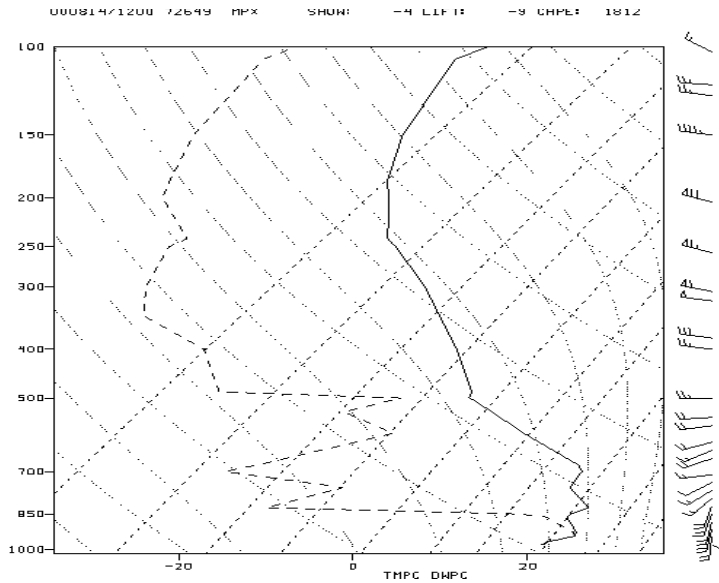


Fig 4. 850 hPa geopotential heights (solid lines), temperature (dashed line, every 5°C) and isotachs (shaded >20 kts). Times as in Figure 3.



(a)



(b)

Fig. 5. (a) 14/12 Aberdeen, South Dakota (ABR) and (b) 14/12 Chanhassen, Minnesota (MPX) soundings showing temperature ( $^{\circ}\text{C}$ )(solid) and dewpoint ( $^{\circ}\text{C}$ )(dashed) on a skew-T – log p diagram. Lifted Index and CAPE are displayed above each sounding respectively.

The surface reflection of these features is shown in Figure 6. At 14/12 (Fig. 6a) a surface low pressure center in northern South Dakota and attendant warm front stretching into southern Minnesota is analyzed. As the surface low moved east during the morning, the surface warm front lifts north and aligns across central Minnesota

into west central Wisconsin. Note that all of the convection during the day occurred along or ahead of the warm front. The surface low and attendant warm front continued to move east into Wisconsin by 15/00 (Fig. 6b).

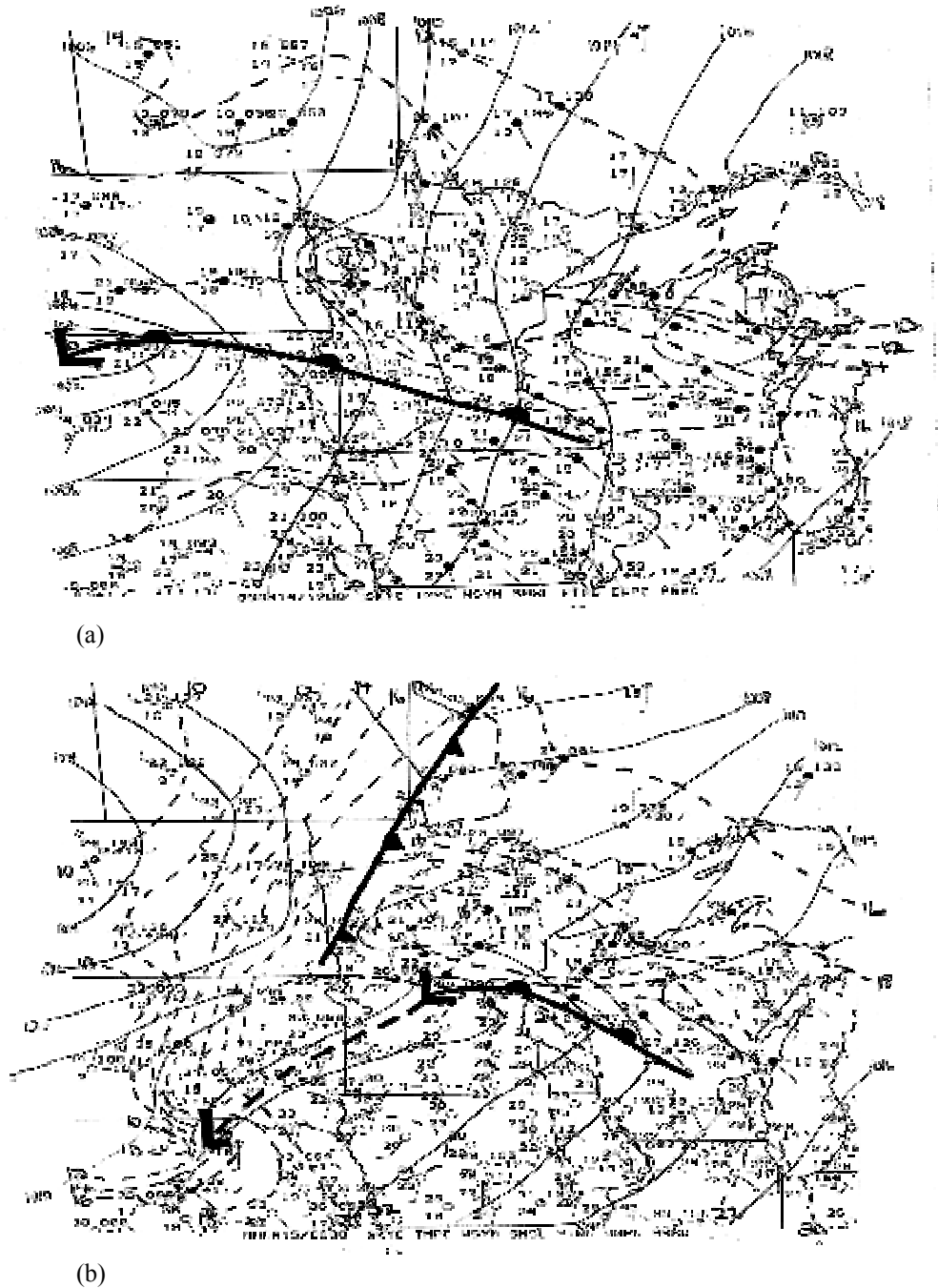
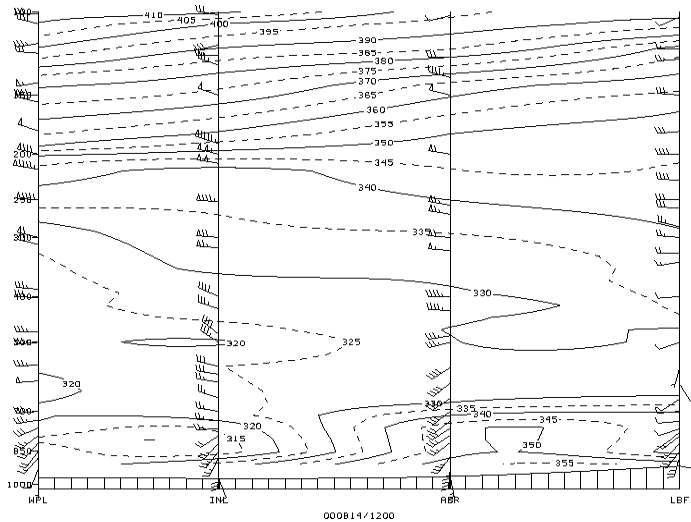


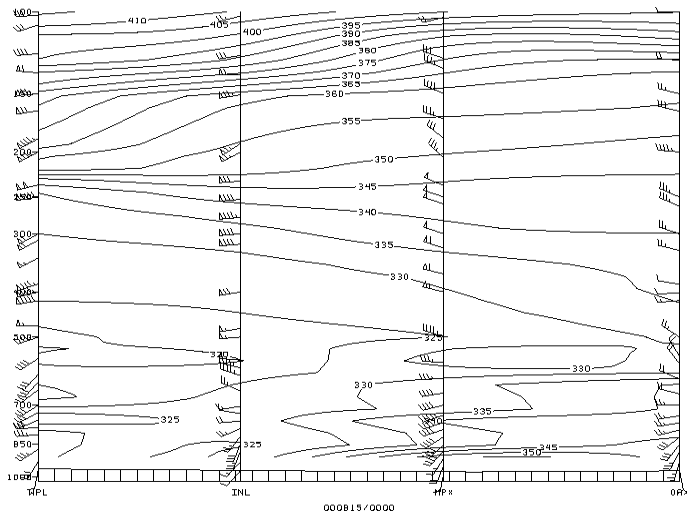
Fig. 6. Manually analyzed surface maps at (a) 14/12 and (b) 15/00. Temperatures are in degrees Celsius and one wind barb is 10 m/s. Isobars (hPa, thin solid lines) are contoured every 2 hPa, and isodrosotherms (dashed lines) are contoured every 2 °C. Note that the most active storm cells occurred just ahead of the surface low pressure center and surface warm front.

c. The convective environment

The 14/12 ABR sounding (Fig. 5a) shows a moist boundary layer overlaid by a relatively dry middle troposphere. A nearly dry adiabatic lapse rate from 850 hPa to 450 hPa yields over 1600 joules of surface-based Convective Available Potential Energy (CAPE) and a Lifted Index (LI) of  $-6$ . The sounding also shows considerable veering from the surface to 800 hPa, implying warm air advection and providing an estimated 65 kts of 0–3 km shear. The Chanhassen, Minnesota (MPX) sounding at the same time (Fig. 5b) shows similar features, although the dry layer is much more pronounced and there is less shear. CAPE and LI values are over 1800 joules and  $-4$  respectively. Both soundings are strongly capped around 850 hPa. A  $\theta_e$  cross section from North Platte, Nebraska (LBF) to Pickle Lake, Ontario at 14/12 (Fig. 7a) shows the convectively unstable atmosphere from LBF to just north of ABR, where the frontal boundary is evident.



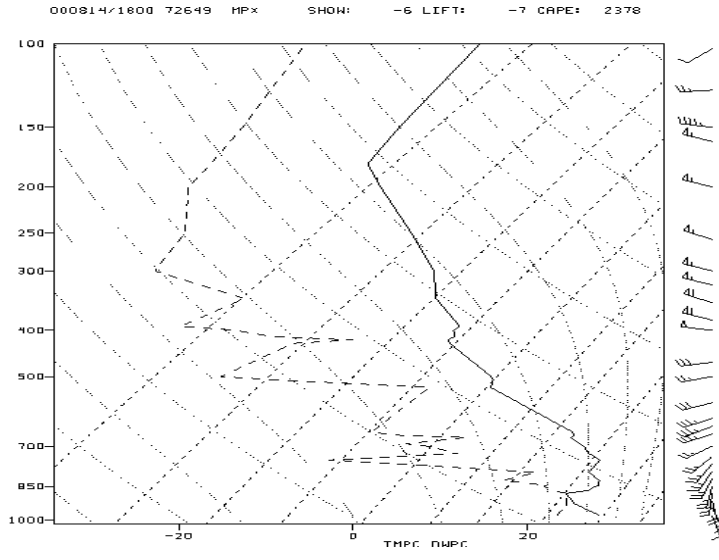
(a)



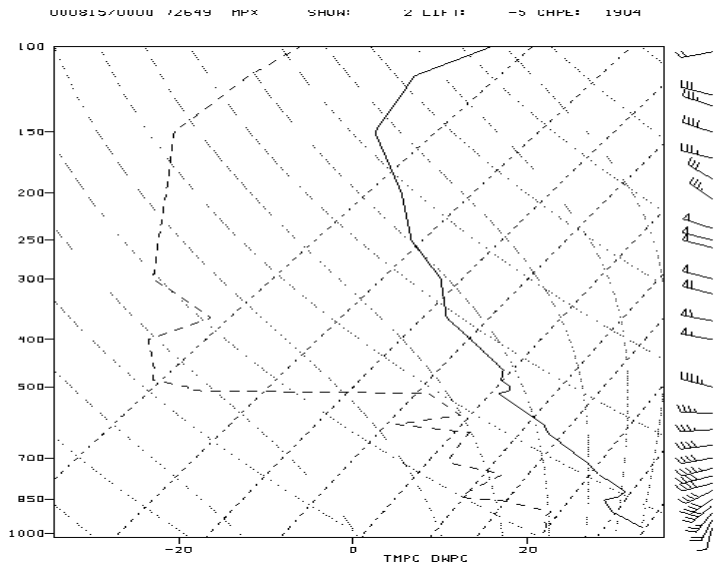
(b)

Fig. 7. (a)  $\theta_e$  cross section from North Platte, Nebraska (LBF) to Pickle Lake, Ontario valid 14/12 and (b) cross section from Valley, Nebraska to Pickle Lake, Ontario valid 15/00. Note the convectively unstable atmosphere from LBF to just north of ABR and MPX respectively.

A special 14/18 sounding from MPX (Fig. 8a) shows the continued destabilization of the lower troposphere as CAPE values are now approaching 2400 joules. However, the atmosphere is well capped with 700 hPa temperatures around 13°C. By 15/00 the MPX sounding (Fig. 8b) continues to show the previously mentioned features with estimated 0-3 km shear of 65 kts; however, it appears surface heating has mixed out the lowest inversion. A  $\theta_e$  cross-section from Valley, Nebraska (OAX) to Pickle Lake, Ontario (WPL) at this time (Fig. 8b) shows a similar profile to the 14/12 profile, with a significant boundary just north of MPX. This boundary is coincident with the southwest flank of the MCC.



(a)



(b)

Fig. 8. (a) 14/18 and (b) 15/00 MPX sounding as in Fig. 6.

#### 4. Analysis of synoptic scale and mesoscale forcing

##### a. Conceptual model

The 14 August event corresponds to the *frontal* synoptic pattern associated with flash floods described by Maddox et al. (1979) (Fig. 9). In this pattern heavy rains occur on the cool side of a slow moving synoptic-scale warm front as warm, convectively unstable air flows over the frontal boundary (Chappell 1986). In most cases a short wave trough approaches the front and stimulates convection. *It was found that these events are distinctly nocturnal* (Maddox et al. 1979; Chappell 1986).

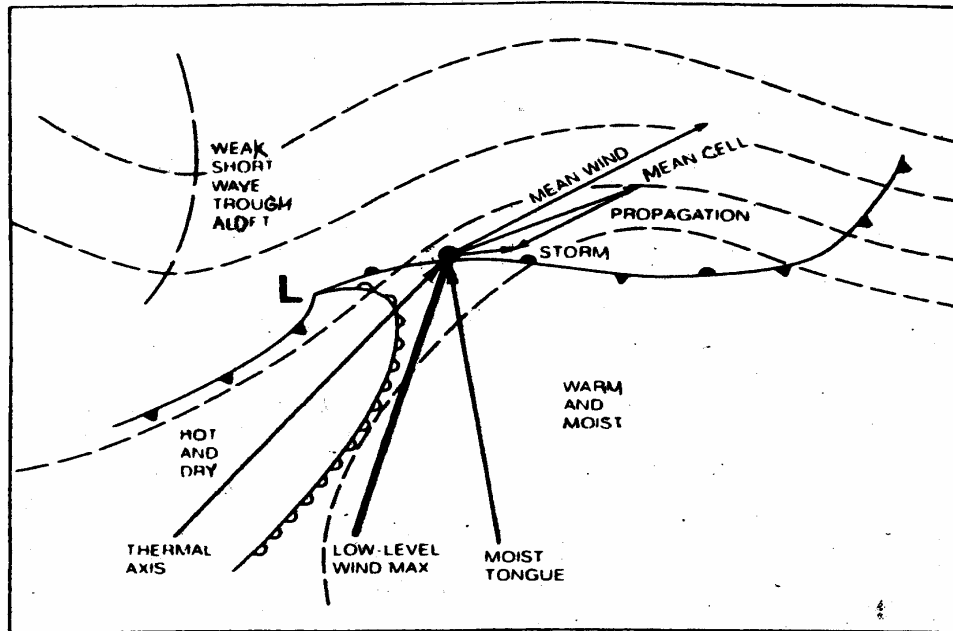
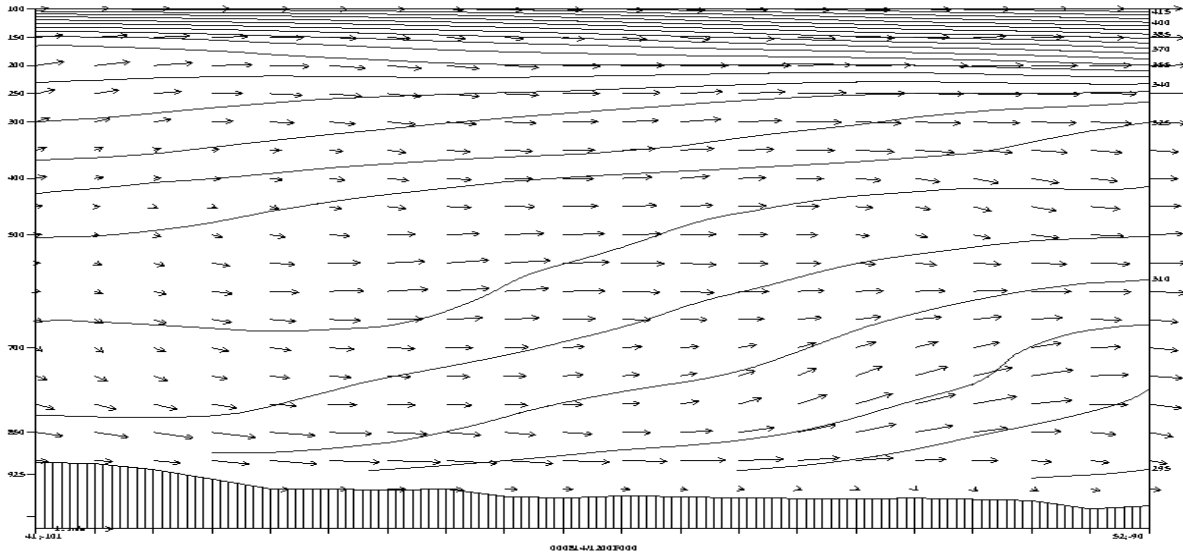


Fig. 9. Frontal type synoptic pattern associated with flash flooding. Note that the storm motion is significantly reduced as new cells continuously reform. (Adopted from Chappell 1986)

Total storm motion has been shown to be the sum of vector mean cell motion and the propagation vector (Chappell 1986; Corfidi et al. 1995). In this pattern coincident maxima of instability and low-level mass and moisture convergence generate periodic cell formation that retards total storm motion (Chappell 1986; Corfidi et al. 1995). Addition of the mean cell and propagation vectors yields a total storm motion that is very slow and directed along the surface front (see Fig. 9). This motion prevents cell downdrafts from destroying the frontal boundary. The rear of the system is favored for continued convection as a flux of moist, convectively unstable air remains available.

Evidence of all synoptic components above are found in the 14 August case. A surface warm front, shortwave disturbance, and convectively unstable atmosphere have been presented above. A  $\theta$  cross-section through the convection at 14/12 (Fig. 10) shows considerable isentropic lift just north of the warm front. This, in addition to cyclonic vorticity advection from the mid-tropospheric short-wave, leads to the lifting of a convectively unstable layer, resulting in deep convection.



LFB

WPL

Fig. 10. Cross section from LFB to WPL of  $\theta_e$  (thin solid lines) and wind and omega tangential to the plane from the 1200 UTC 14 August Eta model initialization. Note the isentropic lift north of the frontal boundary.

Moisture advection, mass convergence, winds and mixing ratio, and moisture flux divergence were calculated from the Eta analysis fields at the 900 hPa level. This level was chosen as it represents the MCC inflow environment best. Plots of moisture advection at 14/12 (Fig. 11, upper left panel), 14/18 (Fig. 12, upper left), and 15/00 (Fig. 13, upper left panel) show significant advection into the southwest sector of the MCC at their respective times. Examination of the winds and mixing ratio (Figs. 11, 12, 13, lower left panels) shows maximums at the exit region of a southerly wind maximum. Similar calculations of mass divergence show significant lower tropospheric convergence in eastern North Dakota and northern Minnesota at 14/12 (Fig. 11a, upper right panel), that shifts south and east to the central Minnesota-Wisconsin border by 15/00 (Fig. 13, upper right panel). Surface convergence was likely enhanced along individual cell outflow boundaries, resulting in periodic cell formation. Significant overlap of moisture advection and mass convergence is coincident with the southwest flank of the MCC at the respective times. Calculations of moisture flux divergence (Figs. 11, 12, 13 lower right panels) quantify this overlap, with maxima correlated with the cell genesis region.

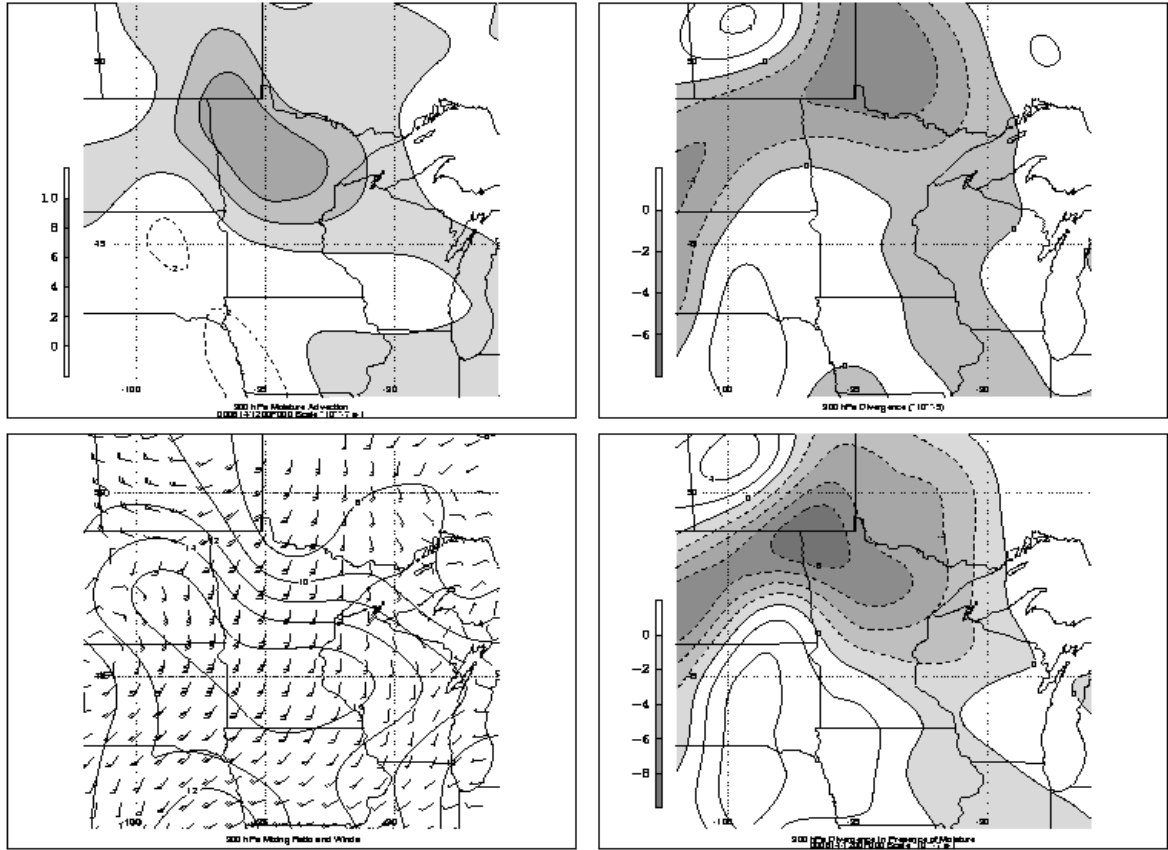


Fig. 11. Four panel plots of 900 hPa moisture advection shaded every  $2 \cdot 10^{-7} \text{ s}^{-1}$  (upper left panel), 900 hPa mass divergence shaded every  $-2 \cdot 10^{-5} \text{ s}^{-1}$  (upper right panel), 900 hPa mixing ratio contoured every 2 g/kg and winds (knots)(lower left panel), and moisture flux divergence shaded every  $2 \cdot 10^{-7} \text{ s}^{-1}$  at 14/1200.

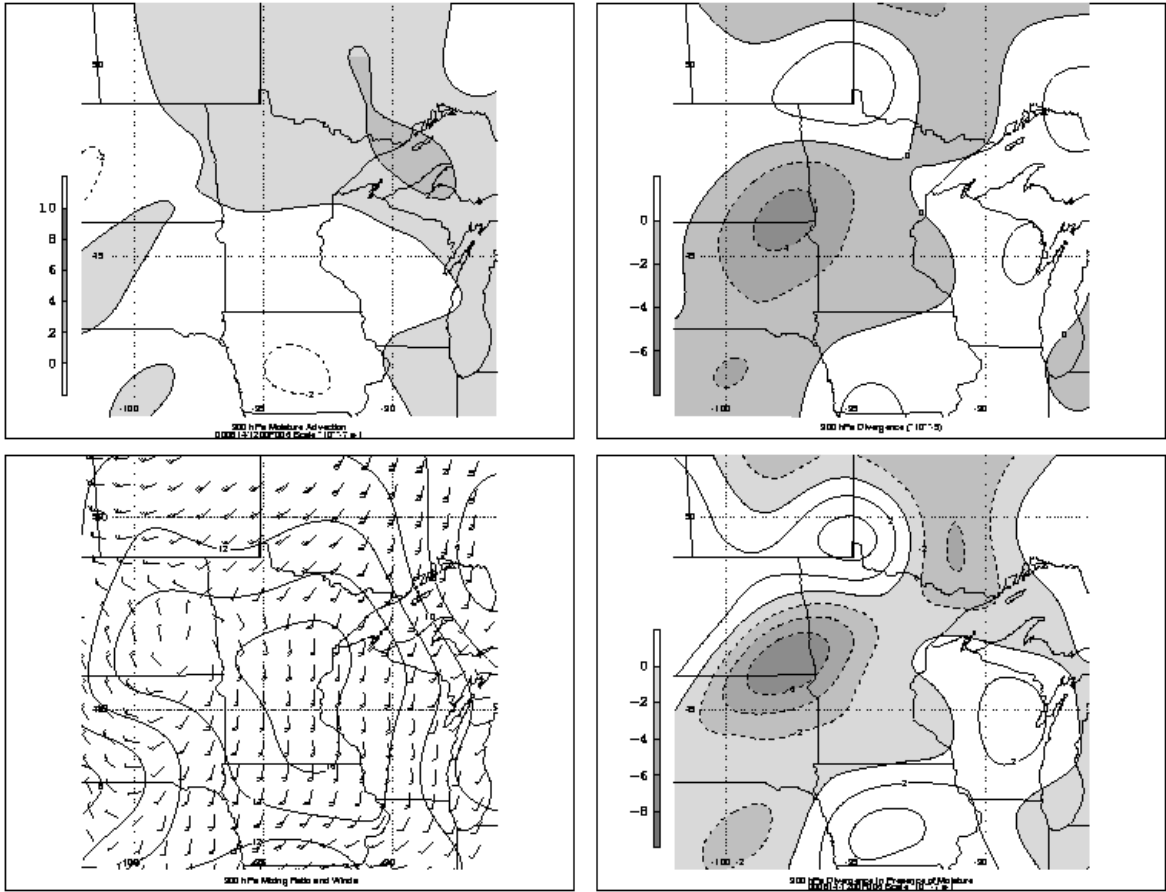


Fig. 12. As in Fig. 11. at 14/18

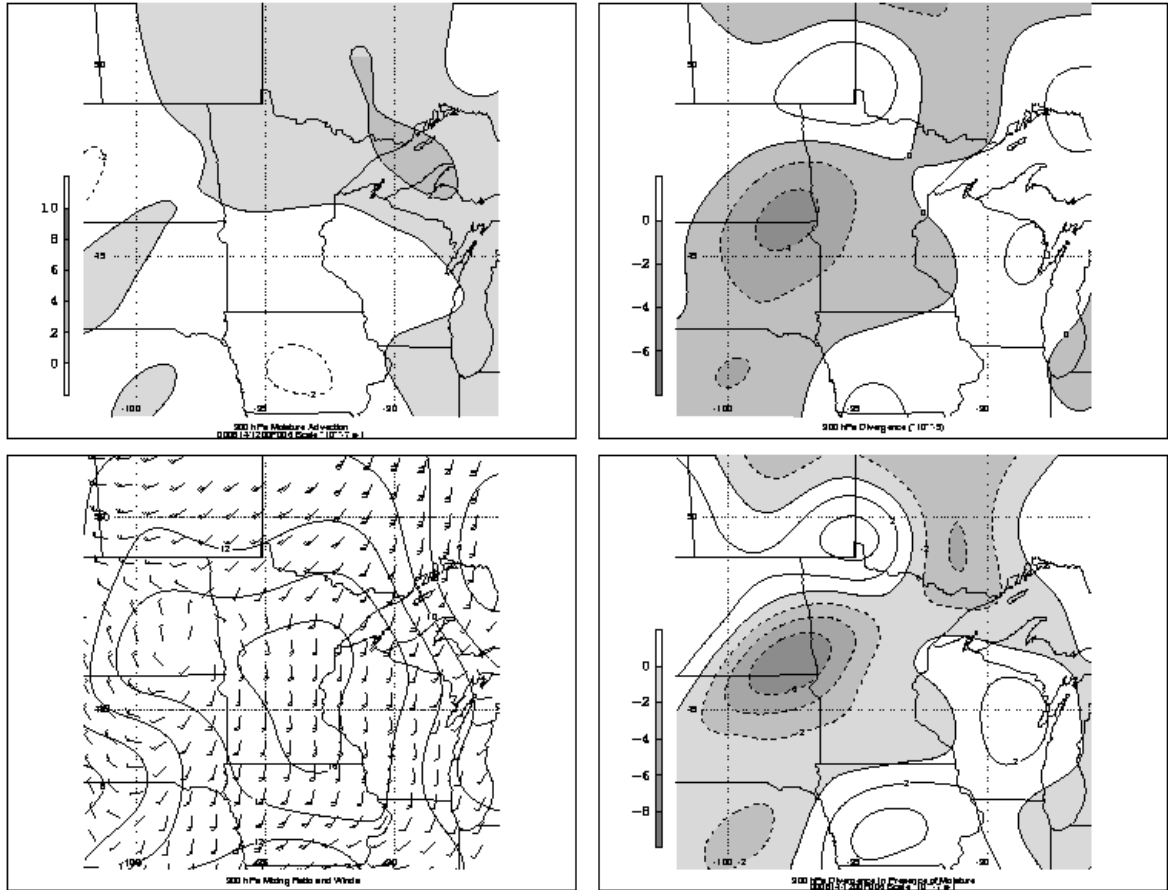


Fig. 12. As in Fig. 11. at 14/18

*a. Storm motion*

The regenerative nature of the convection contributed to the duration of severe weather events and the subsequent warning process. Composite radar loops (not shown) vividly display the rapid individual cell motion to the northeast, with new cells continuously developing towards the southwest, resulting in a slow southeast progression of the system. The rate of new cell formation is dependent on the magnitude of potential energy feeding the cell genesis region, and on the rate it is being replenished. As shown above, significant moisture advection, aided by a low-level wind maxima, was occurring during the system's lifetime.

Corfidi et al. (1995) devised a method to anticipate storm motion incorporating the sum of the mean cell motion and the propagation component. The mean cell motion is derived from the mean flow in the cloud layer. The propagation component has the same magnitude, but is opposite in sign, to the speed and direction of the low-level inflow feeding new cell development (Corfidi et al. 1995). Figure 14 shows the analyzed storm movement derived from radar imagery. Corfidi vectors were manually computed from the ABR sounding data at 14/12, Wood Lake profiler data at 14/18 (Fig. 15), and the MPX sounding data at 15/00. These locations were selected as representative of the low-level storm inflow environment at their respective times.

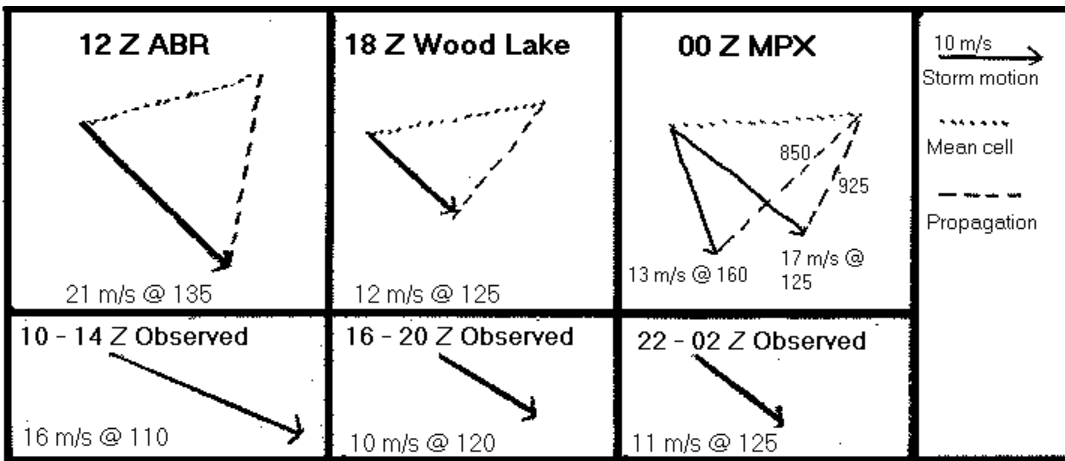


Fig. 14. (top panels) Calculated mean cell motion (short dashed), propagation component (long dashed), and resultant Corfidi vectors (solid) at Aberdeen, South Dakota, Wood Lake, Minnesota, and Chanhassen, Minnesota at respective times. (bottom panels) Radar derived storm motion centered around 12 Z, 18 Z and 00 Z respectively.

Computation of Corfidi vectors using the ABR sounding yielded a storm motion that was quite progressive towards the southeast (21 m/s at 135 degrees). This was attributed to the southerly direction the low level wind maxima. Radar derived storm motion from 14/10 until 14/14 was a comparable 16 m/s at 110°, suggesting the immediate storm environment featured a southwesterly inflow.

Examination of the Wood Lake profiler from 14/15 to 14/21 (Fig. 15) showed a 15 m/s southwest wind at 1500 m. Calculation of Corfidi vectors with this inflow yields a storm motion of 12.5 m/s at 125°. This storm motion is very close to the observed storm motion (10 m/s at 120°).

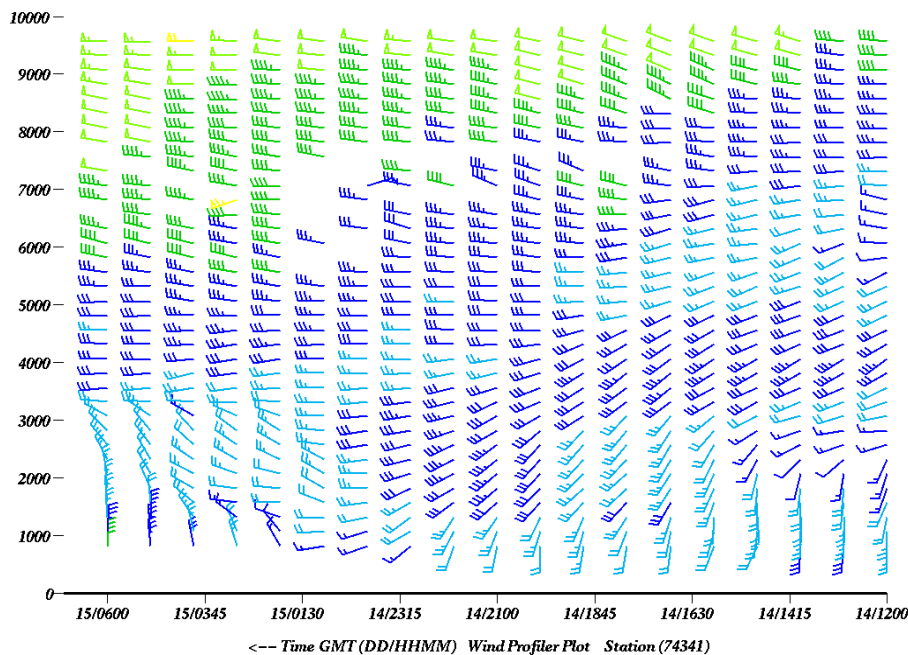


Fig. 15. Wood Lake, Minnesota wind profiler data from 14/12 to 15/06. Height (y-axis) is measured in meters above ground level, and time increases towards the left. Note the strong low-level flow from 14/12 to 14/23. Also note that the character of the profile changes during the late morning as the winds strengthen above 1500 m.

The 15/00 MPX sounding wind data shows a general increase in wind speed with height through the troposphere. In this situation the Corfidi method calls for using the 850 hPa wind vector. However, close examination of the sounding reveals that the 850 hPa level lies at the base of an inversion with a marginal dew point (8 °C) (see Fig. 8b). It seems unlikely moisture fluxes of this magnitude could account for the observed rainfall. Calculation of the Corfidi vector using the more moist 925 hPa level results in a vector speed exceeding the observed storm motion, but in a direction nearly identical to the storm motion (Fig. 15).

Although the observed storm motion and the Corfidi vectors were not identical, the data do show a slower movement than the mean cell motion, suggesting strong low-level inflow created the potential for regenerative storm growth. Forecasters using the Corfidi method in this case could anticipate a slowing of the system during the morning, and predict a southeast storm motion.

## 5. Discussion

The 14 August event conforms to the conceptual model presented by Maddox et al. (1979) in many respects. However, the time phase difference of the event is not accounted for.

The nocturnal preference for MCC development and coincident typical nocturnal maximum in the LLJ has been shown to be physically correlated (Maddox 1983). In the absence of other variables it would appear that the time phase difference of this case (i.e. maximum organization and intensity of convection occurring during the day, instead of at night) could be explained by a LLJ. The regenerative nature of the observed convection also implies the presence of a LLJ, since a significant flux of moist, convectively unstable air was required for the observed rainfall and storm motion.

The nocturnal preference of the LLJ has been shown to be tied to frictional decoupling of the boundary layer during the evening, resulting in super-geostrophic flow (Blackadar 1957). The ABR sounding and morning Wood Lake profiler wind data (Fig. 16) exhibit the distinct signature of this type of forcing since the low level maximum is vertically isolated. Through time the wind profile of the storm inflow maintains low-level magnitude, but also exhibits speed increases above 850 hPa (see Fig. 17). By 15/00 the MPX wind profile shows a general increase in speed with height, with the maximum wind speed around 700 hPa. These wind profiles are *not* signatures of frictional decoupling forcing. Although the forcing of the strong low-level flow was not examined, it appears to be tied to mass adjustment processes forced by synoptic features (i.e. the approach of the shortwave trough, or the secondary circulation of the jet exit region).

Whatever the forcing mechanism, significant fluxes of heat and moisture were nevertheless present during the life cycle of the system. The data suggest that a strong inflow of moist, convectively unstable air into the southwest flank of the MCC was present, and explicitly contributed to the system's longevity. The conceptual model presented by Maddox et al. (1979) and Maddox (1983) presumes traditional forcing of the LLJ (i.e. frictional decoupling of the boundary layer). The strong inflow of this system differed from the conceptual model in that it was *not* a function of boundary layer decoupling. Therefore, the diurnal assumption that the LLJ would weaken during the day did not apply in this case, and fully contributed to the unpredicted nature and magnitude of the system.

## 6. Summary

A synoptic and mesoscale investigation of a MCC was conducted. Analysis revealed it corresponded to the frontal pattern presented by Maddox (1979). However, it was completely out of phase with the conceptual model time frame. Lower-tropospheric examination revealed a strong inflow of moist, convectively unstable air throughout the system's life, which likely sustained the deep convection throughout the day. Corfidi vectors reflect the effect of the low-level wind maxima. Further research is needed to identify the forcing mechanisms responsible for the observed wind maxima

This case illustrates the importance of the LLJ in generating and sustaining MCC convection, regardless of its forcing mechanism, and stresses that care should be taken when applying diurnal assumptions.

### Acknowledgements

We are grateful to the staff of the NWSFO in Duluth, Minnesota for carefully archiving data for this case, especially Norvan Larson who worked the event. Thanks to Matthew Novak for figure drafting. Finally, thanks to the National Weather Service Central Region for technical and editorial assistance, especially Preston Leftwich.

### References

- Augustine, J. A., and F. Caracena, 1994: Lower-tropospheric precursors to nocturnal MCS development over the United States. *Wea. Forecasting*, **9**, 116-135.
- Bosart, L. F. and F. Sanders, 1981: The Johnstown flood of July 1977: A long-lived convective storm. *J. Atmos. Sci.*, **38**, 1616-1642.
- Chappell, C. F. 1986: *Mesoscale Meteorology and Forecasting*, P.S. Ray, Ed., Amer. Meteor. Soc., 296-303.
- Corfidi, S. F., J. H. Merritt and J. M. Fritsch, 1995: Prediction the Movement of Mesoscale Convective Complexes. *Wea. Forecasting*, **11**, 41-46.
- Fritsch, J. M., and R. A. Maddox, 1981: Convectively driven mesoscale weather systems aloft. *J. Appl. Meteor.*, **20**, 9-19.
- Laing, A. G., J. M. Fritsch, 2000: The large-scale environments of the global populations of mesoscale convective complexes. *Mon. Wea. Rev.*, **128**, 2756-2776.
- Maddox, R. A., C. F. Chappell, and L. R. Hoxit 1979: Synoptic and meso-alpha scale aspects of flash flood events. *Bull. Amer. Meteor. Soc.*, **60**, 115-123.
- Maddox, R. A., 1980: Mesoscale convective complexes. *Bull. Amer. Meteor. Soc.*, **61**, 1374-1387.
- , 1983: Large-scale meteorological conditions associated with mid-latitude, mesoscale convective complexes. *Mon. Wea. Rev.*, **111**, 1475-1493.
- McAnelly, R. L., and W. R. Cotton, 1986: Meso-beta-scale characteristics of an episode of meso-alpha-scale convective complexes. *Mon. Wea. Rev.*, **114**, 1740-1770.
- NOAA, 2000: **Storm Data**. Vol. 42
- Wetzel, Peter J., William R. Cotton, and Ray L. McAnelly, 1983: A long-lived mesoscale convective complex. Part II: Evolution and structure of the mature complex. *Mon. Wea. Rev.*, **111**, 1919-1937.